Interlibrary Loans and Journal Article Requests

Proceedings of the ASME 2021
International Mechanical Engineering Congress and Exposition
IMECE2021
November 1-5, 2021, Virtual, Online

IMECE2021-68452

MATHEMATICAL MODELING FOR CARBON DIOXIDE LEVEL WITHIN CONFINED SPACES

Lincan Yan[1], Dave S. Yantek, Cory R. DeGennaro, Rohan D. Fernando

CDC/NIOSH, Pittsburgh, PA, USA

ABSTRACT

Federal regulations require refuge alternatives (RAs) in underground coal mines to provide a life-sustaining environment for miners trapped underground when escape is impossible. A breathable air supply is among those requirements. For built-in-place (BIP) RAs, a borehole air supply (BAS) is commonly used to supply fresh air from the surface. It is assumed that the fresh air has an oxygen concentration of 20.9%. Federal regulations require that such a BAS must supply fresh air at 12.5 cfm or more per person to maintain the oxygen concentration between 18.5% to 23% and carbon dioxide level below the 1% limit specified. However, it is unclear whether 12.5 cfm is indeed needed to maintain this carbon dioxide level. The minimal fresh air flow (FAF) rate needed to maintain the 1% CO_2 level will depend on multiple factors, including the number of people and the volume of the BIP RA. In the past, to predict the interior CO_2 concentration in an occupied RA, 96-hour tests were performed using a physical human breathing simulator. However, given the infinite possibility of the combinations (number of people, size of the BIP RA), it would be impractical to fully investigate the range of parameters that can affect the CO_2 concentration using physical tests.

In this paper, researchers at the National Institute for Occupational Safety and Health (NIOSH) developed a model that can predict how the %CO_2 in an occupied confined space changes with time given the number of occupants and the fresh air flow (FAF) rate. The model was then compared to and validated with test data. The benchmarked model can be used to predict the %CO_2 for any number of people and FAF rate without conducting a 96-hour test. The methodology used in this model can also be used to estimate other gas levels within a confined space.

Keywords: Confined space, gas concentration, breathing air, mathematical model

NOMENCLATURE

t	time after test starts
x	%CO_2 (by mass) at time t within the confined space
x_0	%CO_2 (by mass) in the atmosphere
ρ	air density within the confined space
m	total air mass within the confined space
G	CO_2 generation rate due to breathing
f	fresh air flow rate
P	air pressure in the confined space
R	universal gas constant
T	air temperature in the confined space
CO_2	carbon dioxide
$\%CO_{2_v}$	CO_2 gas concentration by volume
$\%CO_{2_m}$	CO_2 gas concentration by mass
$\%O_{2_m}$	O_2 gas concentration by mass
$\%N_{2_m}$	N_2 gas concentration by mass
M_{CO_2}:	the molar mass for CO_2 gas
M_{O_2}:	the molar mass for O_2 gas
M_{N_2}:	the molar mass for N_2 gas
MSHA	Mine Safety and Health Administration
NIOSH	the National Institute for Occupational Safety and Health
BIP	built-in-place
RA	refuge alternative
BAS	borehole air supply
FAF	fresh air flow

[1] Corresponding author. Email: LYan1@cdc.gov

1. INTRODUCTION

Human breathing generates a significant amount of carbon dioxide. High levels of carbon dioxide can be extremely hazardous [1]. Carbon dioxide mitigation methods, such as soda lime carbon dioxide scrubber curtains and purging with high volume air flows, can prevent carbon dioxide levels from reaching dangerous levels. This is especially critical for confined spaces, such as refuge chambers—also known as refuge alternatives (RAs)—that federal regulations require in underground coal mines to provide miners with a life-sustaining environment in case of an inescapable mine disaster [2] [3]. According to federal regulations, the average carbon dioxide concentration in the occupied structure shall not exceed 1.0%, and excursions shall not exceed 2.5% while maintaining the oxygen concentration between 18.5 and 23%. A 1.0% carbon dioxide (CO_2) atmosphere is the threshold of a serious health risk [2] [3]. The 15-minute short-term exposure limit (STEL) for carbon dioxide set by the National Institute for Occupational Safety and Health (NIOSH) and the American Conference of Governmental Industrial Hygienists (ACGIH) is 3% [4]. Therefore, excursions to 2.5% carbon dioxide must be mitigated quickly.

While occupied and without a breathable air supply, the RA interior oxygen level will decrease, and the carbon dioxide level will increase quickly due to breathing [5]. For built-in-place (BIP) RAs, one mitigation strategy is to implement a borehole air supply (BAS) to supply fresh air from the surface. Federal regulations require the supply of fresh air of 12.5 cfm or more per person to maintain the oxygen and carbon dioxide levels within the safety range as specified in the RA regulations [2] [3]. While the oxygen level is mainly determined by the fresh air flow rate, the CO_2 concentration within the RA will depend on multiple factors including the number of occupants, the volume of the BIP, and the fresh air flow (FAF) rate. The CO_2 concentration can exceed the 1% limit even the oxygen level is within the 18.5% - 23% range. It is crucial to estimate or predict the CO_2 concentration before the RA or other confined being occupied.

In this paper, researchers at NIOSH developed a model that can predict the %CO_2 within an occupied confined space. The model was then compared and validated with test data. The benchmarked model was used to predict the %CO_2 given the number of people and FAF rate without conducting physical test. The methodology used in this model can also be used to estimate other types of gas levels within a confined space.

2. MATHEMATIC MODELING

As illustrated in Figure 1, a confined space has an inward fresh air flow. The confined space is also equipped with a pressure relief valve which allows air to release to outside of the space when the internal pressure reaches the set point of the relief valve. The variables involved in determining the carbon dioxide concentration are defined as in the Nomenclature section. Two models were developed to represent the change in %CO_2 over time. The simplified model relies on a number of assumptions to provide an approximation of the %CO_2 level. The differential model uses differential equations to more accurately represent the change in %CO_2 over time. In the following sections, these two models are described.

2.1 Simplified model

At the point when the test starts, $t=0$, $x=x_0$, and the total CO_2 mass within the confined space is mx_0. As shown in Figure 1, there are two sources that bring CO_2 into the confined space: the fresh air flow and the breathing. There is one outward flow that allows CO_2 to exit the confined space through the exhaust pipe. It is reasonable to assume that the amount of the air exiting the space equals the amount of air entering the space, i.e., the outward air flow rate and inward air flow rate both have a value of f. At time t, the total CO_2 mass, mx, within the confined space is given by

$$m\,x = m\,x_0 + x_0\,f\,t + G\,t - \mu\,x\,f\,t \tag{1}$$

Where μ is a coefficient to average the %CO_2 (by mass) value from time $t=0$ to time t, $0 < \mu < 1$. Consider $x_0 \to 0$, (1) can be rewritten as:

$$x \approx \frac{Gt}{m + \mu f t} \tag{2}$$

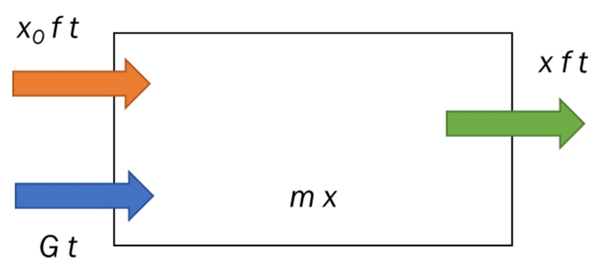

Figure 1. The gas (CO_2) movement into and out of a confined space (dimension of $a \times b \times c$) with fresh air flow. The CO_2 gas moving into the confined space includes breathing (blue) and fresh air flow (orange). The CO_2 gas moves out of the confined space through the exhaust pipe (green).

2.2 Differential model

Define x_{ini} as the initial %CO_2 by mass in the confined space. At the point when the test starts, $t=0$ and $x=x_{ini}$ (refer to Figure 1). For a small time interval, $\Delta t = t_2 - t_1$, the CO_2 mass change within the confined space from t_1 to t_2 is given by:

$$\Delta(mx) = \Delta(Gt + x_0 f t - x f t) \tag{3}$$

Equation (3) can be rewritten as:

$$m\Delta x = G\Delta t + x_0 f \Delta t - x f \Delta t \tag{4}$$

Let $\Delta t = dt \to 0$, then $\Delta x = dx \to 0$. Equation 4 can be rewritten as:

$$mdx = Gdt + x_0 f dt - x f dt \tag{5}$$

$$m\frac{dx}{dt} = G + x_0 f - xf \tag{6}$$

$$m\, x'(t) + f\, x(t) = G + x_0 f \tag{7}$$

Equation (7) is the boundary value problem with the boundary condition: $x(t = 0) = x_{ini}$. Equation (7) is the mathematical and accurate description of the event. Solving the boundary value problem above will give the analytical solution of *x* as a function of *t*.

3. TEST SETUP

In order to conduct testing to examine the CO_2 levels inside an occupied confined space, a test lab was created using a 20-ft-long by 8-ft-wide by 8-ft-high shipping container and a human breathing simulator (HBS) was created to consume oxygen and generate CO_2 to represent human breathing. For the HBS, the concept was to burn propane at the rate necessary to match the rate of human oxygen consumption. Because burning propane generates less CO_2 than human breathing for a set oxygen consumption rate, supplemental CO_2 would have to be added to match both oxygen consumption and CO_2 generation.

To create the HBS, a commercially available propane smoker was modified, and additional test equipment were used to create a well-controlled combustion device. A sealed combustion chamber was created by sealing the bottom of the propane smoker to the floor of the shipping container. Propane was delivered to the sealed combustion chamber from tanks stored outside the shipping container via a gas line that passed through a pressure regulator and a propane mass flow controller. An air pump was used to deliver air from inside the shipping container to the sealed combustion chamber via an airline that was connected to an air mass flow controller. The mass flow rate of propane was determined based on the desired number of people to represent. The air mass flow rate was set 20% higher than the rate needed to provide enough oxygen to support complete propane combustion. To match the CO_2 generation, supplemental CO_2 was provided from a cylinder outside the test lab. A CO_2 mass flow controller was used to provide the additional CO_2 needed to match the CO_2 generated by people.

A previously developed pressure relief valve test stand (PRVTS) was used as the source of fresh air. The PRVTS uses a centrifugal fan connected to a variable frequency drive (VFD) to allow for adjustment of the fresh air provided to the test lab. The PRVTS uses a VELTRON airflow measurement station to measure the provided volume flow of air corrected based on standard atmospheric conditions. The VFD keypad was used to set the FAF to the desired value for a given test.

Multiple gas monitors were used to measure the $\%CO_2$ and $\%O_2$ inside the test lab. To measure the $\%CO_2$, two CTI GG-CO_2 carbon dioxide sensors were positioned within the shipping container. The two sensors were located approximately 6 inches and 3 inches from the floor and positioned around 6.5 feet and 13 feet from the end-wall of the laboratory, respectively. To measure the $\%O_2$, two Macurco OX-6 oxygen sensors were positioned approximately 6 inches and 3 inches from the floor and positioned around 6.5 feet and 13 feet from the end-wall of the laboratory, respectively. One additional O_2 monitor was positioned near the air pump to document the $\%O_2$ in the combustion air.

To record the FAF rate, the CO_2 concentrations, and the oxygen concentrations, a Data Translation DT-9874 data acquisition system was used. All data were recorded at a sample rate of 2 samples per second with 24-bit resolution.

Multiple steps were taken to ensure research safety during the tests. The propane delivery line and the interior of the HBS were checked with a gas leak detector before lighting the propane burner. A Beacon 800 gas monitoring system with multiple CO_2 sensors, an O_2 sensor, a carbon monoxide sensor, and % lower explosive limit sensor was used to ensure all gases within the test lab were at safe levels. If the gas levels exceeded predetermined levels, the Beacon 800 would activate an audible alarm to alert researchers. The presence of a flame in the HBS was monitored using a flame detector and a video camera. If the flame went out, the flame detector would activate an audible alarm and automatically turn off the propane flow via a solenoid valve. Gas monitors at the data acquisition table were used to ensure the O_2, CO_2, CO, and propane levels were at safe levels.

For each test, all flow rates were set based on an assumed number of occupants. The propane flow rate was set based on the rate needed to consume the oxygen of the assumed number of occupants. The combustion air flow rate was set at 1.2 times the air flow rate needed to provide sufficient oxygen to achieve complete combustion. The supplemental CO_2 flow rate was set based on the total CO_2 generation of the assumed number of occupants less the CO_2 generated due to burning propane. The FAF provided by the PRVTS was varied to examine the resulting CO_2 concentration for FAF rates based on dividing the RA regulation requirement of 12.5 cfm per person by integer values from 2 through 7. For each FAF rate, individual tests were conducted until the $\%CO_2$ inside the test lab stabilized.

The CO_2 concentration was measured using two carbon dioxide sensors located within the shipping container. The average $\%CO_2$ was calculated from the readings of the two sensors. All the gas concentrations in Section 3 and Section 4 were either measured or calculated by volume. However, the gas concentration in this section was denoted by mass. For CO_2, the volume concentration relates to the mass concentration through

$$\%CO_{2_v} = \frac{\%CO_{2_m}/M_{CO_2}}{\frac{\%O_{2m}}{M_{O_2}} + \frac{\%N_{2m}}{M_{N_2}} + \frac{\%CO_{2m}}{M_{CO_2}}} \tag{8}$$

where

$\%CO_{2_v}$: the CO_2 gas concentration by volume

$\%CO_{2_m}$: the CO_2 gas concentration by mass

$\%O_{2_m}$: the O_2 gas concentration by mass

$\%N_{2_m}$: the N_2 gas concentration by mass
M_{CO_2}: the molar mass for CO_2 gas
M_{O_2}: the molar mass for O_2 gas
M_{N_2}: the molar mass for N_2 gas.

4. RESULTS

A series of tests was conducted for various numbers of people and FAF rates to observe the CO_2 concentration within the confined space (the shipping container). The first run of the test was to look at the $\%CO_2$ by volume with 40 people and various FAF rates. Two FAF rates were chosen, one low rate (100 cfm) and one high rate (500 cfm). Since the air flow meter did not have the capacity of measuring flow rate below 100 cfm, a large number of people (in our case, a higher propane burning rate to simulate more human breathing) was selected in order to bring down the FAF rate/person.

The first test was to look at the $\%CO_2$ level at various FAF rates for 40 people. The $\%CO_2$ test data was plotted in Figure *2* for FAF rates of 100 cfm (Figure *2*a) and 500 cfm (Figure *2*b). For 40 people and 100 cfm, the FAF rate is 2.5 cfm/person. For 40 people and 500 cfm, the FAF rate is 12.5 cfm/person. The model prediction of $\%CO_2$ value was also plotted and compared with test data in Figure *2*. The figure clearly shows that for both the low FAF rate and high FAF rate, the differential model agrees with test data better than the simplified model. Both the test data and the differential model prediction show that the $\%CO_2$ reaches a steady level in about one hour. For the high FAF rate (500 cfm), the test data and the differential model show the $\%CO_2$ reaches a steady level within 15 minutes.

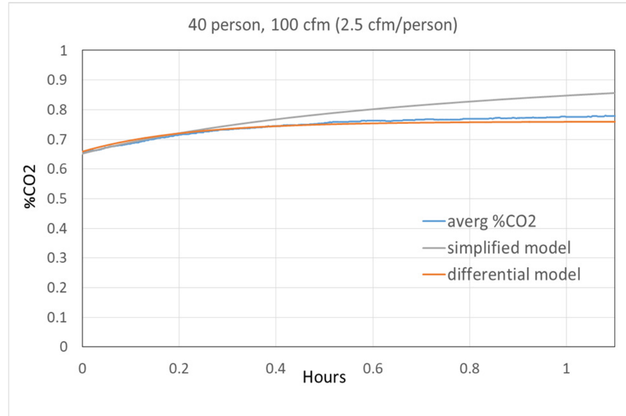

(a)

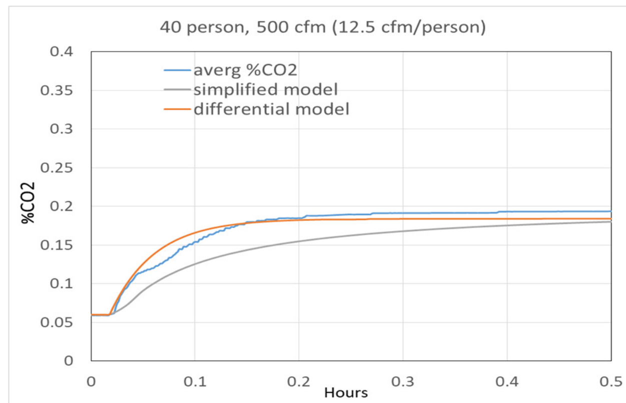

(b)

Figure 2. The $\%CO_2$ (by volume) based on test data and model prediction for 40 people and 100 cfm (a) or 500 cfm (b) FAF rate.

Another test was conducted for 48 people, with FAF rates of 120 cfm and 600 cfm. The $\%CO_2$ test data was plotted in Figure *3* for FAF rates of 120 cfm (Figure *3*a) and 600 cfm (Figure *3*b). For 48 people and 120 cfm, the FAF rate is 2.5 cfm/person. For 48 people and 600 cfm, the FAF rate is 12.5 cfm/person. The predicted $\%CO_2$ values based on the simplified model and the differential model were also plotted and compared with test data in Figure *3*. Again, the figure shows that the differential model predicts the $\%CO_2$ value better than the simplified model. For 120 cfm (Figure *3*a), both the test data and the differential model show that the $\%CO_2$ would reach a steady level within one hour. For 600 cfm (Figure *3*b), both the test data, the simplified model, and the differential model show that the $\%CO_2$ would reach to a steady level within 0.5 hour.

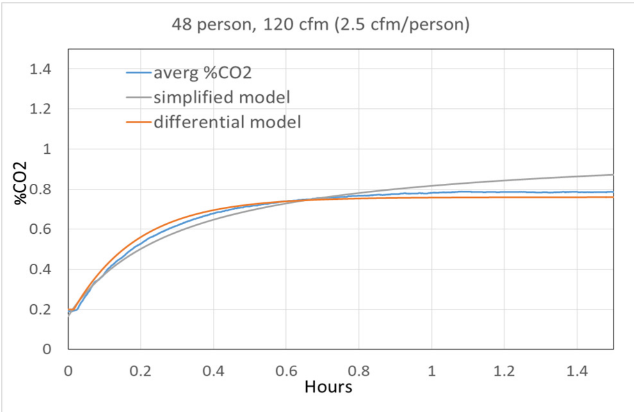

(a)

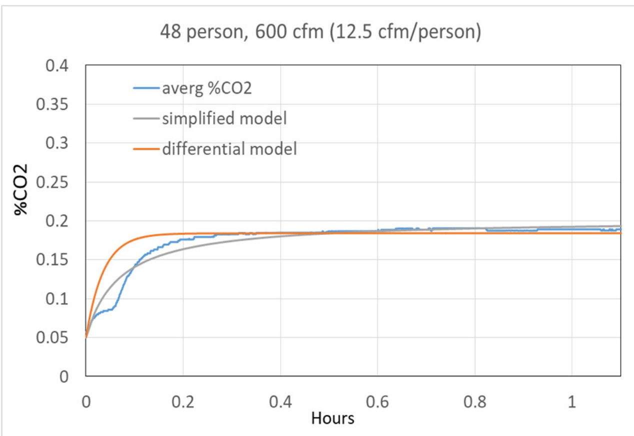

(b)

Figure 3. The $\%CO_2$ (by volume) based on test data and model prediction for 48 people and 120 cfm (a) or 600 cfm (b) FAF rate.

The test data and the differential model show that for FAF rates higher than 2.5 cfm/person, the $\%CO_2$ level within the shipping container will stabilize below 1% (Figure *2* and Figure *3*).

An additional test was conducted with smaller cfm/person value (less than 2.5 cfm/person) by increasing the number of people. Figure *4* shows the differential model validated by test data for 58 people with 105 cfm (Figure *4*a) and 725 cfm (Figure *4*b) FAF rate. For 58 people, the FAF rate is 1.81 cfm/person for 105 cfm and 12.5 cfm/person for 725 cfm.

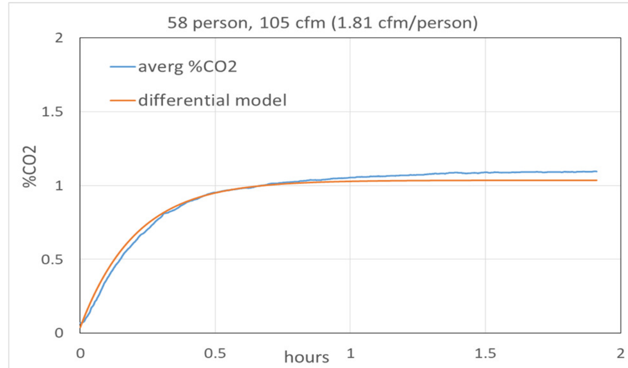

(a)

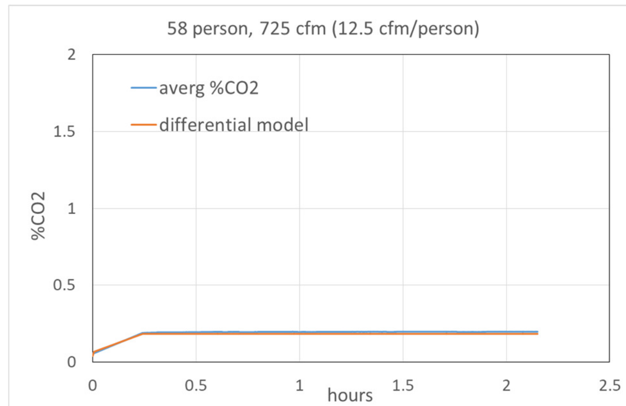

(b)

Figure 4. The $\%CO_2$ (by volume) based on test data and model prediction for 58 people and 105 cfm (a) or 725 cfm (b) FAF rate.

5. DISCUSSION

While fresh air was delivered to the shipping container, the interior pressure would increase until the exhaust valve opened to release the air out. When stabilized, the differential pressure gauge read about 0.3–0.5 inch-of-water (74.7–124.4 Pa) of the interior air pressure. The interior air temperature also increased due to propane burning. It could reach to ~85°F (302.6°K) from ambient temperature (~75°F or 297°K) when the test started. For ideal gas (air),

$$P = \rho RT = \frac{m}{abc} RT \qquad (9)$$

where P is the air pressure, R is the universal gas constant, T is the air temperature, and ρ is the air density.

Equation (9) can be rewritten as:

$$m = \frac{Pabc}{RT} \qquad (10)$$

The pressure fluctuation has a range of 0.074% – 0.123%. The temperature fluctuated at about 1.89% [(302.6°K-297°K)/297°K]. So, the total air mass m should have a fluctuation less than 1.89% due to interior air pressure and temperature increasing. It is reasonable to assume the total air mass remained the same during the test and the pressure/temperature fluctuation can be ignored.

Another observation based on Figure *2*–Figure *4* is that the steady state %CO_2 level depended on the cfm/person value rather than the number of people or the total FAF rate, given other parameters are unchanged. For example, the %CO_2 level stabilized at ~0.8% for 2.5 cfm/person as shown in Figure *2*a and Figure *3*a, regardless of the number of people and the total FAF rate.

Figure 5 shows the %CO_2 predicted by the differential model for various number of people and total FAF rate. The model predicted that the %CO_2 level will approach to 1% for 60 people and 110 cfm or 54 people and 100 cfm. The simulation results for the minimum FAF rate for different numbers of people to maintain %CO_2 < 1% are listed in Table 1. The model predicts the minimal FAF rate to maintain 1% CO_2 to be ~1.87 cfm/person, regardless of the number of people and the total FAF rate.

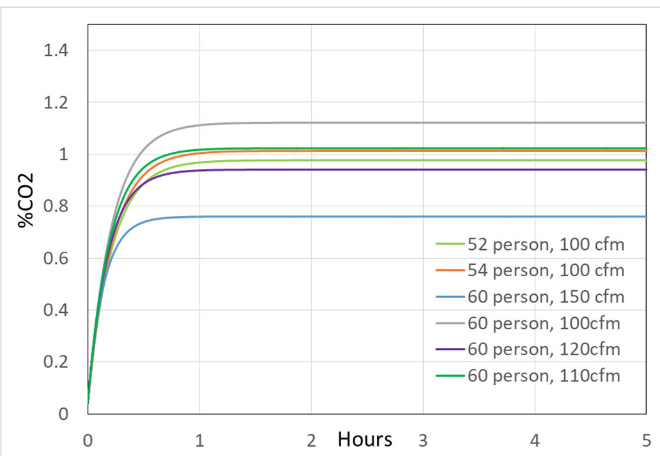

Figure 5. The %CO_2 by volume predicted by the differential model for various numbers of people and FAF rates.

Table 1. The simulation results for the minimum FAF rate for different numbers of people to maintain %CO_2 < 1%.

N	Federal regulation of CFR FAF at 12.5 cfm/person (cfm)	Model Min FAF for CO_2 < 1% (cfm)	Model Min FAF for CO_2 < 1% (cfm/person)
1	12.5	NA	NA
54	675	101	1.87
55	687.5	103	1.87
56	700	105	1.88
57	712.5	107	1.88
58	725	108	1.86
59	737.5	110	1.86
60	750	112	1.87

6. CONCLUSION

The mathematical models presented in this study agree with test data well. They can be used to predict the %CO_2 level based on the parameters of confined space such as the dimension of the confined space, the number of occupants, and the FAF rate. The differential model predicts that a FAF of about 1.87 cfm/person is needed for the %CO_2 to stabilize below 1%. However, safety factors must be taken into consideration when implementing regulations [3]. Because of that, the minimal FAF of 12.5 cfm specified in federal regulations is indeed needed to maintain this carbon dioxide and other gases level within the safe range for 96 hours. The model also predicts the %CO_2 level will reach to steady state within 1 hour or less. Another observation is that the %CO_2 level depends on the cfm/person value rather than the number of people or the total FAF rate. Additionally, the %CO_2 level is more sensitive to the total FAF rate variation than to the number of people.

The benchmarked model can be used to predict the %CO_2 for various numbers of occupants, size of the confined space, and FAF rate without conducting a 96-hour test for every scenario. The model and testing confirm 12.5 cfm of supplied air will sustain miners for 96 hours and comply with the federal regulations. The model may also be useful to help manufacturers and mines to make decisions on RA design and implementation to comply with federal regulations.

DISCLAIMER

The findings and conclusions in this paper are those of the authors and do not necessarily represent the official position of the National Institute for Occupational Safety and Health, Centers for Disease Control and Prevention. Mention of any company or product does not constitute endorsement by NIOSH.

REFERENCES

[1] P. Harper, J. Wilday and M. Bilio, "Assessment of the major hazard potential of carbon dioxide (CO_2)," Health and Safety Executive, 2011.

[2]MSHA, "Regulatory Economic Analysis For Refuge Alternatives For Underground Coal Mines," U.S. Department of Labor, Mine Safety and Health Administration, Office of Standards, Regulations, and Variances, 2008.

[3] MSHA, "30 CFR Parts 7 and 75; Refuge alternatives for underground coal mines; final rule," U.S. Department of Labor, Mine Safety and Health Administration, 2008.

[4]NIOSH, "Occupational Exposure Limits," [Online]. Available: https://www.cdc.gov/niosh/topics/flavorings/limits.html. [Accessed 2018].

[5]E. Bauer, T. Matty and E. Thimons, "Investigation of purging and airlock contamination of mobile refuge alternatives," National Institute for Occupational Safety and Health (NIOSH), 2014.

Proceedings of
ASME 2021 International Mechanical Engineering Congress and Exposition

(IMECE2021)

Volume 13

November 1-5, 2021
Virtual, Online

Conference Sponsor
American Society of
Mechanical Engineers

THE AMERICAN SOCIETY OF MECHANICAL ENGINEERS
Two Park Avenue * New York, N.Y. 10016

ISBN: 978-0-7918-8569-7

INTERNATIONAL MECHANICAL ENGINEERING CONGRESS & EXPOSITION

Dear Distinguished Attendees:

Welcome to the ASME 2021 International Mechanical Engineering Congress and Exposition (IMECE)! We are excited about this year, and continue to celebrate the **breadth**, **depth**, and **technical connections** that are the heart of a worthwhile conference experience. As you consider your schedule for this week, I personally invite you to benefit from each of these aspects of IMECE.

Breadth: 1350+ Technical papers and presentations over 14 technical tracks. At IMECE you can meet with experts from across the spectrum of mechanical engineering research and development. So, spend some time attending a few sessions outside of your technical area and see what you can take back to improve your own work.

Depth: Scientific expertise, not a trade show. From Nobel Laureates to one of the world's most cited researchers, the exceptional research depth at IMECE is nowhere so apparent as in the Congress-Wide Keynote Speakers and the Track Plenaries. For example:

- Dr. Shuji Nakamura, 2014 Nobel Laureate in Physics (Congress-Wide Keynote)
- Dr. Shery Welsh, Director of AFOSR with $500M in Basic Research (Aerospace Track Plenary)
- Dr. Nancy Sottos, Member of the NAE (Materials Track Plenary)
- Dr. Mehrdad Zangeneh, Founding Director of Advanced Design Technology, Ltd (Fluids Track Plenary)
- Dr. Yi Cui, one of the world's most cited scientists (Materials Track Plenary)

And these are just a few of the amazing speakers that will be available to you! Go to (https://event.asme.org/IMECE/Keynote-Speakers) and (https://event.asme.org/IMECE/Program/Track-Plenary) for the full list.

Technical Connections: 2,000+ attendees. The primary benefit of a conference is in meeting and interacting with fellow technical experts. As worldwide health conditions have forced us to remain virtual for a second year, we have implemented several new approaches to enable those interactions, and I invite you to fully participate. Our technical sessions have increased time scheduled for introductions and conversation before, during, and after the technical presentations (pre-recorded with live Q&A). And we have introduced a new series of special technical panels and roundtables designed to be technically focused informal gatherings. Topics for these 30–60-minute sessions range from "Nuclear Power in Space Applications: Promise, Practice, and Challenges" to "New Trends in Lung Therapies" to "Why Thermal Properties Still Matter", to "Advanced Manufacturing Education", "Beyond GPS: Advancing MEMS/NEMS Sensors for Inertial Navigation Only" and many more. The full list of Roundtables and Special Panels are on the congress website. Of course, nothing happens until you push the button. So, please join us! Whether in a technical session or special technical event, Turn on your camera, make a comment, ask a question, share an opinion, and build those connections!

Finally, on behalf of the IMECE Congress Steering Committee, I express my sincere thanks to and recognition of the hundreds of volunteers and the ASME staff that have dedicated time and effort to strengthening the fields of Mechanical Engineering R&D through organizing and leading sessions, topics, and tracks at this year's IMECE. It is never convenient to serve, and we have all continued to face frustrations of schedule, deadlines, conference websites, and more. Thank you for your service. Your efforts have resulted in a strong congress that will continue to drive research forward both now and in the next generation. Thank you.

Sincerely,

Marriner H. Merrill, PhD
IMECE 2021 Technical Program Chair
Materials Science and Technology Division, US Naval Research Laboratory

STEERING COMMITTEE

Marriner Merrill
Technical Program Chair
U. S. Naval Research Laboratory

Dumitru (Micky) Caruntu
Technical Program Vice Chair
University of Texas – Rio Grande Valley

Chris Depcik
General Conference Chair
University of Kansas

Alberto Cuitino
Steering Committee Vice Chair
Rutgers – The State University of New Jersey

Olesya I. Zhupanska
Steering Committee Chair
University of Arizona

Stephen D. Tse
Steering Committee Senate Chair
Rutgers – The State University of New Jersey

Rama Koganti
Steering Committee Senate Member
University of Texas Southwestern Medical Center

Assimina Pelegri
Steering Committee Senate Member
Rutgers – The State University of New Jersey

George Kardomateas
Steering Committee Senate Member
Georgia Institute of Technology

Aaron Knobloch
Steering Committee Senate Member
GE Research

Albert Ratner
Member At Large
University of Iowa

Wenbin Yu
Member at Large
Purdue University

CONFERENCE ORGANIZERS

Acoustics, Vibration, and Phononics
Chair: Yongfeng Xu, *University of Cincinnati*
Co-Chairs:
Guoliang Huang, *University of Missouri*
Mostafa Nouh, *University at Buffalo*

Advanced Manufacturing
Chair: Chetan Nikhare, *Pennsylvania State University, Behrend*
Co-Chairs:
Muhammad Jahan, *Miami University*
Scott Thompson, *Kansas State University*
Yifei Jin, *University of Nevada, Reno*

Advanced Materials: Design, Processing, Characterization and Applications Chair: Hareesh Tippur, *Auburn University*
Co-Chair: Caglar Oskay, *Vanderbilt University*

Advances in Aerospace Technology
Chair: Erkan Oterkus, *University of Strathclyde*
Co-Chairs:
Pavana Prabhakar, *University of Wisconsin-Madison*
Uttam Chakravarty, *University of New Orleans*

Biomedical and Biotechnology Engineering
Chair: Linxia Gu, *Florida Institute of Technology*
Co-Chairs:
Ahmed Al-Jumaily, *Auckland University of Technology*
Martin Tanaka, *Western Carolina University*
Reuben Kraft, *Pennsylvania State University*

Design, Systems, and Complexity
Chair: Miri Weiss-Cohen, *Braude College of Engineering*
Co-Chairs:
Daniele Regazzoni, *University of Bergamo*
Marco Rossoni, *Politecnico di Milano*

Dynamics, Vibration, and Control
Chair: Micky Caruntu, *University of Texas-Rio Grande Valley*
Co-Chairs:
Eleonora Tubaldi, *University of Maryland*
Marco Amabili, *McGill University*

Energy
Chair: Hohyun Lee, *Santa Clara University*
Co-Chairs:
Michael Nistas, *National Technical University of Athens*
Reza Lakeh, *California State Polytechnic University, Pomona*
Soumik Banerjee, *Washington State University*

Engineering Education
Chair: Subha Kumpaty, *Milwaukee School of Engineering*
Co-Chairs:
Anabela Alves, *University of Minho*
Salim Azzouz, *Midwestern State University*

Fluids Engineering
Chair: Philipp Epple, *Coburg University of Applied Sciences*
Co-Chair: Kamran Siddiqui, *Western University*

Heat Transfer and Thermal Engineering
Chair: Ravi Annapragada, *Carrier Corporation*
Co-Chairs:
Alex Rattner, *Pennsylvania State University*
Kevin Dowding, *Sandia National Laboratory*

Mechanics of Solids, Structures, and Fluids
Chair: Marco Amabili, *McGill University*
Co-Chair: Celia Reina, *University of Pennsylvania*

Micro- and Nano-Systems Engineering and Packaging
Chair: Namwon Kim, *Texas State University*
Co-Chair: Gregory Hader, *Stevens Institute of Technology*

Safety Engineering, Risk and Reliability Analysis Chair:
Andrey Morozov, *University of Stuttgart*
Co-Chairs:
Alba Sofi, *University Mediterranea of Reggio Calabria*
Bill Munsell, *Munsell Consulting Services*
Ernie Kee, *University of Illinois Urbana-Champaign* Jennifer S. Cooper, *Boeing*
John Wiechel, *SEA, Ltd.*
Mihai Diaconeasa, *North Carolina State University*
Zahra Mohaghegh, *University of Illinois Urbana-Champaign*

ASME Undergraduate Expo
Chair: Eleonora Tubaldi, *University of Maryland*

NSF
Chair: Siddiq Qidwai, *National Science Foundation*
Co-Chair: Marriner Merrill, *U. S. Naval Research Laboratory*

Research Posters
Chair: Omid Askari, *West Virginia University*
Co-Chairs:
Al Ratner, *University of Iowa*
Dorrin Jarrahbashi, *Texas A&M University*

REVIEWERS

Armin Abbasalinejad
Behrokh Abbasnejad
Moustafa Abdelhamid
Peter Abdo
Hasanain Abdulhadi
Arif Abdullah
Olayinka Abegunde
Kingsley Abhulimen
Omar Aboul-Enein
Mohammad Abshirini
Seena Abu
Zuruzi Abu Samah
Ma'moun Abu-Ayyad
Mohammed Abushamleh
Oyetunde Adeaga
Victor Adegboye
Solomon Adera
Adedotun Adetunla
Pashupati Adhikari
Ashfaq Adnan
Hassan Agalit
Michael Agarana
Ankush Aggarwal
Francesco Aggogeri
Vivek Agnihotri
Vipin Agrawal
Ebenezer Ahiati
Furqan Ahmad
Narendra Akhadkar
Bakytzhan Akhmetov
Murat Aksu
Hani Al Hazmi
Abdullah F. Alajmi
Fahd Alam
Mohammad Didarul Alam
Sheymaa Alazzawi
Muhamed Albadawi
Tyler Albright
Saleh Alhumaid
Ammar Ali
Abdulaziz Alkandari
Rami Alkhatib
Seyed Allameh
Brendon C. Allen
Mohammed Al-Mudhafar
Moza Alnaimi
Gioacchino Alotta
Saif Alrafeek
Mohammad Al-Rawi
Saja Al-Rifai
Saad Alshahrani
Ahmad Alshorman
Ahmed Alshwairekh
Anabela Alves
Sachin Alya
Marco Amabili
Rohan Amare
Catherine Ambrose
Ali Ameri
Alberto Amerini
Saeb AmirAhmadi Chomachar
Alireza Amirkhizi
Feruza Amirkulova
Luling An
Nadish Anand
Nishita Anandan
Kevin Anderson
Mohanish Andurkar
M. Anthony Xavior
Enrico Antonini
Noble Anumbe
China Rama Lakshman Anumolu
Eyyup Aras
Egemen Aras
Emanuele Vincenzo Arcieri
Tariq Arif
Aaron Armstrong
Alberto Arroyo
Muzammil Arshad
Muhammad Arslan
Rmanathan Arunachalam
Utsav Raj Aryal
Asaed Asaed
Rasoul Askari
Omid Askari
Mohamad Aslani
Md Saifuddin Ahmed Atique
Mystica Augustine Michael Duke
Stefan aus der Wiesche
Vikrant Aute
Kleio Avrithi
Mohsen Ayoobi
Saeed Azad
Martin Azese
Saad Aziz
Yousof Azizi
Salim Azzouz
Gnanavel B.K.
Alireza Babaei
Ridha Baccouche
Daniel Bacellar
Mehar Bade
Amit Bagchi
Johnny Bahri
Xin Bai
Christopher Bailey
Emerson Baker
Amirhamed Bakhtiarydavijani
Sayavur Bakhtiyarov
Ashok Bakshi
Alla V. Balueva
Arkasama Bandyopadhyay
Deb Banerjee
Portia Banerjee
Anjishnu Banerjee
Arnab Banerjee
Richa Bansal
Hua Bao
Corina Barbalata
Gustavo Barbosa

Erik Bardy
Brett Barker
Deibys Barreto
Mike Barringer
Gaurav Bartarya
Akinsanya Damilare Baruwa
J. Sadhik Basha
Muhammad Anser Bashir
Mary Bastawrous
Anirban Basudhar
Riccardo Becchi
Andrew Bellocchio
Roberto Belotti
Alberto Benato
Mohammed El Khalil Bendadi
Ryan Berke
Michael Beyer
Kiran Bhaganagar
Anantha Padmanabhan Bhagavatheeswaran
Pranav Bhounsule
Luigi Biagiotti
Linkan Bian
Cosimo Bianchini
Michele Bici
Joseph Bickson
Kazi Md Masum Billah
Christopher Billings
Joseph Bishop
Sayan Biswas
Nolan Black
Joseph Blochberger
James Bluman
Saran Srikanth Bodda
Sandra K.S. Boetcher
Brian T. Bohan
Giacomo Bonaccorsi
Carlos Borras Pinilla
Andrea Botta
Sebastiaan Bottenheim
Nikolaos Bouklas
Charbel Bou-Mosleh
M'Hamed Boutaous
Andrew Bowman
Gulcharan Brainch
Michael Brambley
Ivan Breslavsky
Nathan Brinkman
Alexander Brown
Antonio Bula
Clayton P. Byers
Shengze Cai
Ercan Cakmak
Zhen Cao
Yihan Cao
Yue Cao
Roberto Capata
Martina Capone
Giovanni Carabin
Luca Carbonari
Van Carey
Gianluca Carraro
Dumitru Caruntu
Jennifer Case
Osvaldo Castro
Pietro Catalano
Paride Cavallone
Oana Cazacu
Emrah Celik
Cesar Celis
David Cereceda
Wadie Chalgham
Edwin Chan
Nitin Chandola
Yanni Chang
Fernando Charrua-Santos
Arka P. Chattopadhyay
Somnath Chattopadhyay
Sergei Chekurov
Shawn Chen
Jie Chen
Jianli Chen
Leitao Chen
Haodong Chen
Jinwei Chen
Yilun Chen
Shu Chen
Guang Chen
Zhiyi Chen
Qun Chen
YungChia Chen
J.S. Chen
Daniel Chen
Jiangtao Cheng
Meng-Sang Chew
John Chew
Sheng-Wei Chi
Eric Chia
Manohar Chidurala
Rahul Chikurde
Peter Childs
Geetha Chimata
Abhijeet Chodankar
Junseo Choi
Jae-Won Choi
Paolo Cicconi
Lee Clemon
Lorenzo Cocchi
Kristin Cody
David Cohen
John Collinger
Giorgio Colombo
Filippo Colombo Zefinetti
Jennifer Cooper
Casey Corrado
Sol-Carolina Costa
John Cotter
Bryce Cox
Daniel Cox
Nathan Crane
Ricardo Cuenca-Alvarez
Zheng Cui
Shuang Cui
Anthony D Angelo
Shweta Dabetwar
Huwei Dai
Zhaohe Dai
Manab Kumar Das
Himanshu Dave
Michael Davidson

Ethan Davis
Shuvodeep De
Robert Dean
Ibrahim Deiab
Phillip Deierling
Xin Deng
Shikai Deng
Onur Denizhan
Scott DePaula
Christopher Depcik
Ryan DeWall
Pankaj Dhaka
T.S. Dhanasekaran
Marco Di Bartolomeo
Davide Di Battista
Mihai A. Diaconeasa
Joao Dias
Gerardo Diaz
Jerrold Dietz
Sheng Ding
Siyi Ding
Sunil Dingare
Aniruddha Dive
Nicholas DiZinno
Xiangyang Dong
Janet Dong
De Dong
Pei Dong
Pengfei Dong
John S. Donnal
Sushil Doranga
Haley Doude
James Downs
Xianping Du
Zhidong Du
Shawn Duan
Christopher Dumm
Christopher Duron
Debarun Dutta
Sandip Dutta
Anjali Dwivedi
Shiyuan E.
Arjun Earthperson
Williams Ebhota
Paul Egan
Stephen Ekwaro-Osire
Francisco Elizalde Blancas
Raed El-Jawahri
Mohamed Elsayed
Mahmoud Elsharafi
William Emblom
Doctor Enivweru
Philipp Epple
Jayakiran Reddy Esanakula
Roja Esmaeeli
Mehdi Esmaeilpour
Kandula Eswara Sai Kumar
John Evans
Tagir Fabarisov
Danial Faghihi
Tanvir Faisal
Y. Fan
Yin Fan
Liwu Fan
Jun Fang
Xiaomin Fang
Saman Farhangdoust
Amirhossein Farvardin
Milad Farzad
Mahsa Farzaneh
Arianna Fatahi
Fabio Fatigati
Olawale Fatoba
Claudio Favi
Shaw Feng
Jinyang Feng
Naheed Ferdous
Fábio Fernandes
Svitlana Fialkova
Robin Fisher
David Flodman
C.S. Florio
Laurie Florio
Tyler Flynn
Victor Manuel Fontalvo Morales
Emine Foust
Claiton Franchi
Giulio Franchini
Michael Frazier
Emma Frosina
Gen Fu
Konda Reddy G.
Xiang Gao
Yuan Gao
Qian Gao
Pedro De Jesus García Zugasti
Zacharias Garza
Andrew Gaynor
Ozhan Gecgel
David Gee
Takele Gemeda
Joshua Gess
Levon Ghabuzyan
Amin Ghadami
Aref Ghaderi
Hamed Ghaffari
Fadi Ghaith
Mohsen Ghamari
Samad Gharehdaghi
Suhash Ghosh
Dipannita Ghosh
Anthony Giachin
Duncan William Gibbons
James Gibert
Antoni Gil Pujol
Axel Glahn
Emmanuel Glakpe
Aneesha Gogineni
Nathaniel Goldfarb
Yiska Goldfeld
Humberto Gomez Vega
Ugrasen Gonchikar
Stefano Gonella
Hernando Gonzalez
Arturo González
Germanico Gonzalez Badillo
Kalyan Goparaju

Yimy. Gordon
Recep M. Gorguluarslan
Ravi Gorthala
James Griffin
Tyler Grimm
Philipp Grimmeisen
Yaroslav Grosu
Chenchen Gu
Linxia Gu
Yuyang Gu
Shuitao Gu
Peng Guan
Guillermina Guerrero
David Guirguis
Rasim Guldiken
Amol Gulve
Yu Guo
Hong Guo
Zongqi Guo
Yang Guo
Zheng Guo
Tanuj Gupta
Anuj Gupta
Aniket Gupta
Sonam Gupta
Srinivasa Rao Gurrala
Sathish Kumar Gurupatham
Khan Habeeb Ur Rahman
Grzegorz Hader
Noah Hafner
Bhuiyan Shameem Mahmood Ebna Hai
Salim Haidar
Taher Hajilounezhad
Henry Haley
Peter Hamlington
Mostafa Hamza
Mohamed Hamza
Li-Hsin Han
Hai-Chao Han
Julie Hao
Matt Harrison
Mostafa Hassanalian
Pezhman Hassanpour
Grant Hawkes
Andrew Hayden
Jiaze He
Kai He
Rui He
Ge He
Nathaniel Heathman
Cole Hefner
Anwar Hegazy
James Heidmann
Michael Hennessey
Daniel Herber
Tomas Hermansson
Abel Hernandez-Guerrero
Blake Herren
Morteza Heydari
Juan Luis Higuera-Trujillo
Michael Hillman
Mohammad Hodaei
Wyatt Hodges
John Homer
Peyman Honarmandi
Senhao Hou
QiTao Hou
Jiacheng Hou
Linzao Hou
Larry Howlett
Quang-Cherng Hsu
Yuhang Hu
Ming Hu
Kui Hu
Weijian Hua
Cathy Huang
Guoliang Huang
Bradley Huddleston
Hugo Hultman
Gabriele Humbert
Matti Huotari
Mahmoud Hussein
Parsaoran Hutapea
Gisuk Hwang
Lee Hyun Jae
Matthew Iannacci
Stephen Idem
Patricia Iglesias Victoria
Zeki Ilhan
Danny Illera Perozo
Miho Ishii-Teshima
Saif Mohammad Ishraq Bari
Nazmul Islam
Mahmudul Islam
Didi Istardi
Teruaki Ito
Brian D. Iverson
Anthony Izaguirre
Nathan Jackson
Suchana Akter Jahan
M.P. Jahan
José Jimmy Jaime Rodríguez
Abhishek Jain
Ankur Jain
Divya Jaladi
Hadi Jalali
Tausif Jamal
Sagil James
Ricardo Jardim-Goncalves
Esam Jasim
Carolina Jauregui
Sanjib Jaypuria
Robabeh Jazaei
T.R. Jebieshia
Selvaraj Jegadheeswaran
Songbai Ji
Xiaoxu Ji
Weiqi Ji
Yikai Jia
Tao Jia
Xiaoning Jiang
Zhiyuan Jiang
Zhu Jiang
Xin Jin
Jianhang Jin
Yifei Jin
Xusheng Jing
Jeanne Joachim

Mathew John
Murray Johnston
Matthew Jones
Michael Jonson
Sung-hwan Joo
Kris Jorgensen
Hamed Kalami
Onur Can Kalay
Hisham Kamel
Nitin Kamitkar
Kiana Kamrani Fard
K Kanishk
Sathish Kannan
Daniel Kaplan
Anargyros A. Karakalas
Kostas Karazis
Fernando Karg Bulnes
Soroor Karimi
Amir Karimi
Shashank Karra
Bright Katey
Ernest Kee
Eugenia Kennedy
Fardin Khalili
Jobaidur Khan
Mohammad Khan
Sufia Khatoon
Ryan Khawarizmi
Lyes Khezzar
Namwon Kim
Hanseul Kim
Seunghee Kim
Byungki Kim
Jungho Kim
Dongsu Kim
Hyun Jin Kim
Dohwan Kim
Owen Kingstedt
Vidya Kishore
Janardhan Kodavasal
Pratik Koirala
Kranthi Kolli
Jason Kolodziej
Teja Konduri
Behrad Koohbor
Matthew Korey
Satyanarayana Kosaraju
Basavraj Kothavale
Nitin Ramesh Kotkunde
Reuben Kraft
James Kribs
Nitin Nagesh Kulkarni
Rajesh Kumar
Deepak Kumar
Anil Kumar
Subha Kumpaty
Robert Kunz
Jim Kuo
Harsha Kusnoorkar
Vladimir Kuts
Sang Muk Kwark
Reza Lakeh
Ritesh Lakhkar
Prasanth Anand Kumar Lam
Asheesh Lanba
Daniele Landi
Horst Lanzerath
Michael Lapera
Curt Laubscher
William Lawrimore
Xiaobin Le
Francesco Leali
Michael Leamy
E.J. LeBlanc
Elias Ledesma Orozco
Juhyeong Lee
Chang-Chun Lee
Ho-Hoon Lee
Moo-Yeon Lee
Hohyun Lee
Christopher Lee
Peter Lee
Kun-Lin Lee
Taehun Lee
Ming-Tsang Lee
Juyoung Leem
Victor Lefevre
Devanda Lek
Tommaso Lenzi
Yanfei Li
Yongqiang Li
Puxuan Li
Zhichao Li
Xianglin Li
Hua Li
Yaofa Li
Jinglun Li
Yanjun Li
Mingzhe Li
Zhimin Li
Zhiye Li
Zhenxing Li
Gang Li
Tianchu Li
Yumeng Li
Bo Li
Weitao Li
Chao Liang
Hong Liang
Xiong Liang
Theo Lim
Sheng-Min Doris Lin
Zhibin Lin
Jiazhen Ling
Noam Lior
Andrew Littlefield
Haowen Liu
Haidong Liu
Yao-Hsien Liu
Yucheng Liu
Ling Liu
Tao Liu
Xin Liu
Qingchang Liu
Yingtao Liu
Tangzhu Liu
Haijun Liu
Summer Locke
Robert L. Lowe
Saul Loza
Zexi Lu

Qi Lu
Qiyue Lu
Weiyi Lu
Dirk M. Luchtenburg
V.T. Lukong
Sergey Lupuleac
Jianfeng Ma
Zhen Ma
Yuliang Ma
Haibo Ma
David Mabelane
Brianna MacNider
Ebrahim Maghami
Ameneh Maghsoodi
Mohammad Maghsoudi-Ganjeh
Mahboobe Mahdavi
Mohammad Mahinfalah
Kashif Mahmood
Mohammadreza Mahmoudi
Pooya Mahmoudian
Mohammad Mahtabi
Varad Maitra
Dipanjan Majumdar
Yelaman Maksum
Sepehr Maktabi
Rahul Makwana
Subhasish Malik
Mahmood Mamivand
Dilip Mandal
Giovanni Manente
Randall Manteufel
Maurizio Manzo
Jessica Gissella Maradey Lazaro
Jared Marcel
Marco Marconi
Christopher Martin
Jose Israel Martinez Lopez
Roberto Martinez-Montejano
Jeremy Marvel
Matthew Maschmann
Kathryn H. Matlack
Kathryn Maupin
Lorenzo Mazzei
James McCusker
Kevin McMullen
Joshua Mctigue
Tanmoy Medhi
Arash Mehraban
Hil Meijer
Shabbir Memon
Julie Mendez
Gregory Meyer
Tianwei Miao
Siamak Mirfendereski
Kyran Mish
M.P. Mishra
Arpit Mishra
Samy Missoum
Sridhara Rao Mittapalli
Mohand Mohamed
Walid Mohamed
Hamid Mohammadi
Ram Mohan
Lokanath Mohanta
Lesego Mohlala
Vera Moiseytseva
Wael Mokhtar
A.K.M. Monayem H. Mazumder
Keegan Moore
Vito Moreno
Carlos Luis Moreno Negrin
Andrey Morozov
Mehdi Mortazavi
Ershad Mortazavian
Mojtaba Moshtaghzadeh
Fan Mu
Muhammed Muaz
Partha P. Mukherjee
Saptarshi Mukherjee
Subrata Mukherjee
Arun Muley
Rydge Mulford
Manuel Müller
Sungkwang Mun
Troy Munro
William Munsell
Joydeep Munshi
Giuseppe Muscolino
Satish Muthu
Mamoona Muzammil
Avitus Mwelinde
Aggrey Mwesigye
Mahdi Nabil
Rajesh Nagadolla
Moeto Nagai
Shailendra Naik
Kalyani Nair
Hamidreza Najafi
Ali Najafi
Ahmad Najafi
Ahad Nasab
Farshad Navah
Helena Navarro
Kashif Nawaz
Ivaylo Nedyalkov
Ezz El-Din Nehad Mostafa
George Nelson
Samuel C. Neu
Vinh Nguyen
Xinchen Ni
Chetan Nikhare
Pouriya Niknam
Joachim Nilsen Grimstad
Xin Ning
Michail Nitsas
Arman Nokhosteen
Mostafa Nouh
Margaret Nowicki
Saied Nusier
John Nuszkowski
Andrzej Nycz
Aronu Obinna
Gregory Odegard
Hannah O'Hern
Jeong Tae Ok
Andreas Olympios
Sameer Osman

Selda Oterkus
Saad Oudah
Sunday Olayinka Oyedepo
Hakan Ozaltun
Vijay Pachore
Darshan Pahinkar
Rishi Pahuja
Brian Painter
Rajendra Prasath Palanisamy
Kevin Pan
Heng Pan
Kapil Panchal
Hitesh Panchal
Priyanka Pandit
Junru Pang
Amrinder Singh Pannu
Lalit Pant
Alessandra Papetti
John Pappas
Anatoly Parahovnik
P. Parameswaran
Mihir Parekh
Keunhan Park
Chanwoo Park
Hoonmin Park
Omkar Parkar
Maximilian Passmann
Michael Pate
Darshil Patel
Dhiren Patel
Kavi Patel
Sandeep Patil
Brandon Patterson
Uma Maheshwera Reddy Paturi
Brent Paul
Titan Paul
Vivek Pawar
Srinivasa Rao Pedapati
Reza Pejman
Assimina Pelegri
Vladimir Pena
Fang Yu Peng
Edwin Peraza Hernandez
Salman Pervaiz
Mohnish Peswani
Marco Petrolo
Michael Pettes
Tomasz Piatkowski
Roy Pillers
Fabio Pini
Pius Pius
Matthew Plutt
Pranaya Pokharel
Burak Polat
Wilma Polini
Bibek Poudel
Ricardo Poveda
Vinit Prabhu
Jose I. Prado
Raghu V. Prakash
Anchasa Pramuanjaroenkij
Hariyo Priambudi Setyo Pratomo
William Prescott
Cristina Prieto
Ernesto Primera
Prashant Chandra Pujari
Marco Puliti
Mohammad Khairul Habib Pulok
Tuomas Puttonen
Dong Qian
Xin Qian
Dongsheng Qiao
Guangzhao Qin Qin
D. Dane Quinn
Tãµnis Raamets
Hassan Raheem
Peyman Rahimi Borujerdi
S.M. Mahbobur Rahman
Mohammad Rizwen Ur Rahman
M. Shafiqur Rahman
Mahabubur Rahman
Manjunath C. Rajagopal
Anurag Rajagopal
Vomsheendhur Raju
Chandra Sekhar Rakurty
Manoj Ram
Karthikeyan Ramanujam
Vaishak Ramesh Sagar
Angel D. Ramirez
Maria Ramos Gonzalez
Mohammadreza Ramzanpour
Zhongnan Ran
G.M. Rahid Uz Zaman Rana
Nithin Rangasamy
Rakesh Ranjan
Jing Rao
Fayaz Rasheed
Anton Rassõlkin
Shubham Rath
Albert Ratner
Alexander Rattner
Marisha Rawlins
Bahni Ray
Sergio Rech
Daniele Regazzoni
Sambad Regmi
Giulio Reina
Mitchell Rencheck
Ramjee Repaka
Benoit Revil-Baudard
Marcos Reyes-Martinez
Abolfazl Rezaei Aderiani
Elnaz Rezaian
Dong-Ho Rhee
Jovica Riznic
Caterina Rizzi
Nicholas Roberts
Franklin Robinson
Frederico Rodrigues
Marcelo Rodrigues Fernandes
Hee Seok Roh
Ajith Krishnan Rohini
Freddy Jesus Rojas Chavez

David Romero
Cameron Rose
Marco Rossoni
Michael Roth
S. Rouhi
Shrabanti Roy
Arnab Roy
Bikram Roy Chowdhury
Xiulin Ruan
Christopher Rudolf
Eric Ruggiero
David Ruiz
Sangjin Ryu
Lakshmi S.
Ahmed S. Saad
Parisa Saboori
Ibrahim Sabry
Ahsana Sadaf
Roham Sadeghi Tabar
S. Sadeqi
Babak Safaei
Amrit Sagar
Pankaj Saha
Sujoy Saha
Sudipta Saha
Ujjwal K. Saha
Probir Saha
Lokesh Saharan
Iskender Sahin
Bijoyraj Sahu
Muhammed Saif
Anil Saigal
Hani Sait
Roozbeh (Ross) Salary
Khaled Sallam
Santhakumar Sampath
Mauricio Sanchez
Juan Sandoval
Sridhar Santhanam
Kaushik Sarkar
Pratik Sarker
Jyotirmoy Sarma
Robert Saunders
Toshiyuki Sawa
Lorenzo Scalera
Olivia Scheibel
Frank Schieck
Matthew Schifano
Gillian Schiffer
Bryan Schmidt
Anne Schmitz
Adriano Sciacovelli
Majura Selekwa
Rajiv Selvam
Soroush Sepahyar
Michael Sevier
Eduard Ševtšenko
Arash Shadlaghani
Harshal Y. Shahare
Ashu Sharma
Rajeev Sharma
Preet Sharma
Mostafa Shazly
Zhengjing Shen
He Shen
S.A. Sherif
Shuquan Shi
Yuan Shi
Yunye Shi
Jingjing Shi
Tom Shih
Sidney Bruce Shiki
Saeed Shiri
Md. Imrul Reza Shishir
Olalekan O. Shobayo
Jamileh Shojaeiarani
Wan Shou
XueDao Shu
Ashwin Siddarth
Mathieu-Antoine Sierro
João Silva
Abhishek Kumar Singh
Nityanand Sinha
Ashish Sinha
Ahmad Sleiti
Dean Snelling
Rikard Söderberg
Alba Sofi
Ratnak Sok
Abhijit Som
Wangbing Song
In-Hyouk Song
Jinwoo Song
Guangchao Song
Li Song
Zhengyi Song
Xiaolei Song
Hoanan Song
Yooseob Song
Mehmet Sozen
McKay Sperry
Vinod Srinivasan
Rajeshwar Sripada
Ankit Srivastava
Terrin Stachiw
John Steimke
Vesselin Stoilov
Gabriel Streitmatter
Samuel Subia
Harish Subramanyan
Prathik Jain Sudhir
Taylor Suess
C. Steve Suh
Yunyun Sun
Lei Sun
Haining Sun
Wangping Sun
Shung-hsing Sung
Vyshak Sureshkumar
Ehsan Taati
Alireza Tabarraei
Alex Tacescu
Luca Tagliafico
Hossein Taheri
Abdul Raouf Tajik
Siddharth Talapatra
Lorenzo Talluri
Ilie Talpasanu
Atsutaka Tamura
Kwek-Tze Tan
Hua Tan
X. Gary Tan

Martin Tanaka
Hui Tang
Jinsong Tang
Yash Tank
Khalid Tantawi
Buddi Tanya
Akin Tatoglu
Dorothy Taylor
Mehran Tehrani
Khashayar Teimoori
Ayse Tekes
Halil Tekinalp
John Tencer
Zhiqiang Teng
Alp Tezbasharan
Mishal Thapa
Scott Thompson
Zhenhua Tian
Ang Tian
Saeed Tiari
Juan Tibaquira
Ankit Tiwari
Beth Todd
Ravi Pratap Singh Tomar
Mukul Tomar
Robert Tomko
Casey Troxler
Eleonora Tubaldi
Göker Türkakar
Pawan Tyagi
James V. Cox
Luca Valdarno
R. Michael Van Auken
Kenneth Van Treuren
K. Philip Varghese
Thomas Vasko
Kostiantyn Vasylevskyi
Andrea Vecchi
Arun Veeramany
Ruben Venegas
Holalu Venkatdas Ravindra
Chadalavada Venkateswara Babu
Ankit Verma
Riccardo Vescovini
Carlos Ramón Vidal Tovar
Jose L. Viesca
Umberto Villa
Vimal Viswanathan
Andrea Vitali
Diego Vittorini
Kelen Cristiane Teixeira Vivaldini
Gabriele Volpato
Tung Vuong
Anand Vyas
Adam Wachtor
Ian Walker
Graham Walker
D.K. Walters
Xingyu Wang
Michael Cai Wang
Xinwei Wang
Yeqing Wang
Qiming Wang
Jingyu Wang
Wei Wang
Junzhen Wang
Curtis Wang
Zhenyu Wang
Yan Wang
Peng Wang
Jianhua Wang
Wenxi Wang
Shiyan Wang
Xueju (Sophie) Wang
Kristina Warmefjord
Ronald Warzoha
Dane Wedgeworth
Justin Weinmeister
Miri Weiss Cohen
Yi Wen
John Wiechel
Enakshi Wikramanayake
Sara Wilson
Stephanie Wimmer
Keo-Yuan Wu
Zhijun Wu
Chenglin Wu
Mingtao Wu
C.T. Wu
Wenxuan Xia
Yingxiang Xia
Xiao Xiangyu
Xinyi Xiao
Angran Xiao
Gongnan Xie
Zhuowen Xie
Siyuan Xing
Ruitong Xiong
Luoyu Xu
Jun Xu
Yongfeng Xu
Yeyin Xu
Minghan Xu
Tongge Xu
Baoxing Xu
Wei Xue
Reza Yaghmaie
Sami Yamanidouzisorkhabi
Karen Chang Yan
Ling Yan
Lincan Yan
Chen Yan
Zhuo Yang
Chun-Lin Yang
Yichao Yang
Mengqiao Yang
Bingen (Ben) Yang
Haoqing Yang
Song Yang
Shujie Yang
Xiaolong Yang
Weizhu Yang
Zhonghua Yang
Yifei Yao
Wei Yao
Timothy Yap
Taiho Yeom
Ravinder Yerram

Sumith Yesudasan Daisy
Steven Yip Fun Yeung
Ho Yeung
Guilian Yi
Salih Yildiz
Sha Yin
Akio Yonezu
William Young
Kianoosh Yousefi
Cunjiang Yu
Kai Yu
Hong Yu
Zexing Yu
Pengyu Yuan
Chunhao Yuan
Sichen Yuan
Zhangxian Yuan
Andrei Zagrai
Md. Zahid Hasan
Guiyan Zang
Jian Zeng
Chi Zhan
Lufan Zhang
Ning Zhang
Wei Zhang
Lin Zhang
Kaihao Zhang
Yanmei Zhang
Wen Zhang
Zhou Zhang
Zilong Zhang
Jianan Zhang
Xiaoliang Zhang
Jing Zhang
Chao Zhang
Zhifeng Zhang
Xiaoyu Zhang
Liang Zhang
Chen Zhang
Yue Zhang
Jian Zhang
Nathan Zhang
He Zhang
Min Zhang
Yongqing Zhang
Mingshao Zhang
Peiran Zhang
Peter Zhang
Qinqiang Zhang
Haipeng Zhang
Dianyun Zhang
Yating Zhang
Xian Zhang
Man Zhao
Huijuan Zhao
Shijia Zhao
Kai Zhao
Changlong Zheng
Cao Zhi
Allan Zhong
Hong Zhou
Yanguang Zhou
Min Zhou
Zenghao Zhu
Linda Zhu
Linqi Zhuang
Wei Zhuang
Metodi Zlatinov
Hamidreza Zobeiri
An Zou
Ahmad Zueter

CONTENTS

Proceedings of ASME 2021 International Mechanical Engineering Congress and Exposition Volume 13

Safety Engineering, Risk, and Reliability Analysis

Congress-Wide Symposium on Prognostic and Health Management: NDE and Prognostics of Structures and Systems

Crashworthiness, Occupant Protection, and Biomechanics

General Topics on Risk, Safety, and Reliability

Reliability and Safety in Industrial Automation Systems

Reliability and Safety in Transportation Systems

Reliability and Safety of Deep Learning-Based Components

Student Safety Innovation Challenge